Available online at www.sciencedirect.com
SCIENCE DIRECT®
Biochimica et Biophysica Acta 1757 (2006) 798–810
BIOCHIMICA ET BIOPHYSICA ACTA
BBA
www.elsevier.com/locate/bbabio

A micellar model system for the role of zeaxanthin in the non-photochemical quenching process of photosynthesis—chlorophyll fluorescence quenching by the xanthophylls

Shlomo Avital [a], Vlad Brumfeld [b], Shmuel Malkin [a,*]

[a] *Department of Biological Chemistry, The Weizmann Institute of Science, Rehovot, 76100, Israel*
[b] *Department of Plant Sciences, The Weizmann Institute of Science, Rehovot, 76100, Israel*

Received 15 January 2006; received in revised form 8 May 2006; accepted 30 May 2006
Available online 7 June 2006

Abstract

To get an insight to the mechanism of the zeaxanthin-dependent non-photochemical quenching in photosystem II of photosynthesis, we probed the interaction of some xanthophylls with excited chlorophyll-a by trapping both pigments in micelles of triton X-100. Optimal distribution of pigments among micelles was obtained by proper control of the micelle concentration, using formamide in the reaction mixture, which varies the micellar aggregation number over three orders of magnitude. The optimal reaction mixture was obtained around 40% (v/v) formamide in 0.2–0.4% (v/v) triton X-100 in water. Zeaxanthin in the micellar solution exhibited initially absorption and circular dichroism spectral features corresponding to a J-type aggregate. The spectrum was transformed over time (half-time values vary—an average characteristic figure is roughly 20 min) to give features representing an H-type aggregate. The isosbestic point in the series of spectral curves favors the supposition of a rather simple reaction between two pure J and H-types dimeric species. Violaxanthin exhibited immediately stable spectral features corresponding to a mixture of J-type and more predominately H-type dimers. Lutein, neoxanthin and β-carotene did not show any aggregated spectral forms in micelles. The spectral features in micelles were compared to spectra in aqueous acetone, where the assignment to various aggregated types was established previously. The specific tendency of zeaxanthin to form the J-type dimer (or aggregate) could be important for its function in photosynthesis. The abilities of five carotenoids (zeaxanthin, violaxanthin, lutein, neoxanthin and β-carotene) to quench chlorophyll-a fluorescence were compared. Zeaxanthin, in its two micellar dimeric forms, and β-carotene were comparable good quenchers of chlorophyll-a fluorescence. Violaxanthin was a much weaker quencher, if at all. Lutein and neoxanthin rather enhanced the fluorescence. The implications to non-photochemical quenching process in photosynthesis are discussed.

Keywords: Triton X-100; Micelle; Micellar aggregation number; Formamide; β-carotene; Violaxanthin; Zeaxanthin; Lutein; Neoxanthin; Aggregate; Dimer; Circular dichroism; Concentration self-quenching

1. Introduction

Non-photochemical quenching (NPQ) is an important regulatory process in photosynthesis, strategically aimed to diminish any damage, which may be caused by high light intensities [1]. The mechanism of NPQ has been the subject of intensive research (see, e.g., [1–8]). NPQ occurs in photosystem II (PS II), which is particularly prone to light damage [9] and from which emanates most of Chl-*a* fluorescence that serves as an indicator to NPQ [10]. NPQ establishes additional routes for the dissipation of the excitation energy to thermal energy. This diminishes the relative rate of formation of damaging entities [3] (e.g., triplet state Chl-*a* and consequently singlet oxygen), still allowing sufficient excitation to drive the saturation level of electron transport.

There is an association between the appearance of non-photochemical quenching (NPQ), the presence of low pH in the thylakoid lumen produced by photosynthetic electron transport and the formations of zeaxanthin from violaxanthin (the xanthophyll cycle)

Abbreviations: Bchl-*a*, bacteriochlorophyll a; Chl-*a*, chlorophyll a; c.m.c., critical micellar concentration; FA, formamide; HPLC, high pressure liquid chromatography; LHC-II, light harvesting system or light harvesting complex of photosystem II; NPQ, Non-photochemical quenching; THF, tetrahydrofuran; TX-100, triton X-100 (p- (1,1,3,5-tetramethylbutyl) phenoxy polyoxy-ethylene glycol); QELS, quasi-elastic light scattering method

* Corresponding author. Tel.: +972 8 9464093; fax: +972 8 9344118.
E-mail address: shmuel.malkin@weizmann.ac.il (S. Malkin).

0005-2728/$ - see front matter © 2006 Elsevier B.V. All rights reserved.
doi:10.1016/j.bbabio.2006.05.038

[4]. The zeaxanthin dependence led to the assumption that zeaxanthin is involved directly by interacting with chlorophyll in its excited singlet state. Some authors assumed initially [11,12] that the energy of the (spectroscopically silent) first excited singlet state of zeaxanthin is lower than the corresponding state of Chl-*a* so that such quenching occurs by 1S–1S energy transfer. By the same token, the non-ability of violaxanthin to quench was explained by assuming that its lowest excited state energy was higher than that of Chl-*a*. These assumptions were based on the difference in the number of conjugated double bonds of the above carotenoids (9 for violaxanthin and 11 for zeaxanthin), and the corresponding presumed decrease of the energy of the π electron system [12].

Early experimental estimations [13,14] showed, however, that both carotenoids lowest excited singlet states energy levels lie below, albeit close to, the lowest energy state of Chl-*a*, and that the difference between them is not sufficient to explain the differential quenching in-vivo. More recent estimations, closer to an in-vivo situation, were made for some xanthophylls bound to a recombinant protein of the LHC-II family (Lhcb1) [15]. These gave even more similar numbers for the excited state energies of lutein, zeaxanthin and violaxanthin, which were well below that of Chl-*a*. In the latter case zeaxanthin and violaxanthin quenched Chl-*a* fluorescence to the same degree [16]. These discouraging results could mean that the effect of zeaxanthin is indeed not direct and let the above authors to abandon the idea of direct quenching. Their final conclusion was that the specificity of the quenching could not be explained by the photophysical properties of the xanthophylls. Thus, they tended to agree with another view expressed earlier by Horton and his coworkers [17] that specific conformational changes occur in the LHC-II protein, caused by the low lumenal pH and magnified by the bound zeaxanthin, which results in the chlorophyll fluorescence quenching.

Whether a conformational change is a perquisite to NPQ or not, there is still no answer to the actual physical mechanism of the quenching. The idea of a direct interaction between zeaxanthin and Chl-*a* can be still kept, by considering, e.g., a mechanism of charge-transfer for the quenching. Indeed, theoretical considerations indicate such possibility [18,19], which is supported by the recent experimental observation of photoinduced rapid formation of transient zeaxanthin cation under NPQ conditions [20]. A conformational change in the LHC-II could bring zeaxanthin and chlorophyll-*a* to close proximity, allowing their interaction. An alternative hypothesis is that the conformational change may cause two (or more) Chl-*a* molecules to become closely packed and thus serve as a quenching centre [21].

A simple first step to confirm the possibility of direct quenching is to make a straight check on the quenching abilities, in-vitro, of the involved carotenoids on chlorophyll fluorescence. Such experiment was performed with β-carotene, which was shown to be an efficient quencher of Chl-*a* fluorescence in an organic solution [22–24]. Unfortunately, to the best of our knowledge, there is no solid experimental data on the capacity of zeaxanthin, violaxanthin and other xanthophylls as quenchers in-vitro.

At that point we decided to use a micellar system, rather than a simple organic solution, to test the quenching abilities of the xanthophylls. In the last case, effective diffusion-limited dynamic quenching requires to use quite high quencher concentrations, in the mM range, which could lead to undesirable secondary effects. The rational behind the use of the micellar system was the possibility to trap single Chl-*a* and carotenoid molecules in the same micelle, allowing their interaction, at a much smaller overall concentration (in the μM concentration range). This would avoid possible complexities due to the use of high concentrations and significantly economize on the xanthophylls, which are very expensive.

The chosen micellar model system was based on the detergent triton X-100, dissolved in formamide/water mixture. This system, at a fixed formamide (FA) concentration (75%), was used by Rosenbach-Belkin et al. to test the formation of bacteriochlorophyll dimers and higher aggregates [25]. Preliminary experiments in our laboratory demonstrated indeed that in such micelles zeaxanthin is a much stronger quencher of Chl-*a* fluorescence than violaxanthin [26]. Since then, we further developed the micellar system and explored its characteristics and the changes that occur in the spectra of the inserted pigments. In particular, varying the formamide concentration was found to cause unexpectedly very large changes in the micellar size, which in consequence affected the occupation number of the micelles by the inserted pigments. The differential quenching abilities of added carotenoids on Chl-*a* fluorescence were then confirmed under more controlled conditions and optimized. This was documented in a Ph.D. thesis [27].

The results with the micellar system [27] indicated, however, large changes in the spectra of the added zeaxanthin and violaxanthin, caused by their dimerization. This was first discouraging to us, not thinking that they could be relevant to the photosynthetic system. Later, we were encouraged by reports on similar spectral changes in the transition to non-photochemical quenching state in-vivo [28,29], particularly after binding to a specific LHC-II protein (PsbS) [30]—a possible candidate for NPQ site [8]. We now feel that our results may be in harmony with the possibility expressed in these works, that NPQ could be activated by specific zeaxanthin binding to LHC-II, presumably forming a dimer in the aggregated state of LHC-II, which acts as a quencher of excited Chl-*a*. The tendency of zeaxanthin to form dimers and higher aggregates in our model system actually gives an opportunity to check these forms as candidates for chlorophyll fluorescence quenching.

2. Materials and methods

2.1. Chemicals, pigments and preparations

Formamide (FA) and pyridine were of HPLC grade. β-carotene was purchased from Sigma. Zeaxanthin (6-R, 6′-R) was initially obtained as a gift from Hoffman LaRoche (Basel, Switzerland). Other natural pigments (Chl-*a*, violaxanthin, neoxanthin and lutein) were initially extracted from spinach or pea thylakoids. Additional violaxanthin was kindly given to us by Dr. Alexander Ruban. At a later stage Chl-*a* was purchased from Sigma and violaxanthin as well as dimethoxy-zeaxanthin were purchased from CaroteNature (Lupsingen, Switzerland). Carotenoids were in all–trans configuration. The extraction of pigments, HPLC fractionation and identification followed general procedures described in [31] and further detailed in [27].

TX-100 micelles in aqueous solutions were prepared freshly for each day experiments. The micellar mixture is defined as volume parts (v/v) of each component: TX-100 (0.2–0.4%), FA (0–75%) and doubly distilled water. This

mixture was sonicated in an ultrasonic bath cleaner (Laboratory supplies NY, GI 22SPI) at 80,000 Hz and 80 W sonic power. Chl-*a* was added from its pyridine solution and the mixture was further sonicated for 1 min. Oxygen was excluded by continuous argon bubbling during micelle preparation, keeping the micellar mixture under argon until use. Carotenoids were added immediately before the experiments (usually from their pyridine solutions, other solvents were used occasionally). The pyridine concentration in the micelles did not exceed 1.7%.

2.2. Micellar size estimation

The micellar size determines the distribution of pigments among the micelles. Two aspects were measured: the geometric size and the aggregation number, which were found to be FA concentration dependent.

The geometric size was obtained by the quasi-elastic light scattering method (QELS) [32], based on auto-correlation function of laser-light scattering from the micelles. This yields a diffusion constant, which from Einstein–Stokes equation results in an apparent molecular radius. The relative viscosity was estimated as a function of the FA concentration by the method of flow rate and converted to absolute values by comparison to handbook values of pure water and FA. The refractive index was interpolated linearly from the values for pure water and FA. QELS measurements could not be performed in presence of pigments because light absorption perturbed seriously the light scattering measurements.

QELS determination required that the micellar solution should be free from foreign particles. For this, the water used was passed through 0.2 μm micropore filters and the micellar solution was centrifuged for 30 min at 3200×*g*, excepting the solution at 75% FA, which contained very large micelles and centrifuged for only 5 min. The centrifugation eliminated any foreign particles remaining in the water, or introduced from the FA or TX-100 stock materials.

The micellar solution was heterogeneous and the geometric size is expressed as a distribution of hydrodynamic diameters, with amplitudes that tend to overestimate higher diameters. Also, since the larger sized micelles are not spherical, the obtained diameter is an apparent number that gives a rather rough indication to the micellar size as a function of the FA concentration.

The aggregation number (i.e., the number of TX-100 monomers per micelle) was obtained by measurement of the concentration self-quenching of chlorophyll fluorescence [21], which in our case depends on the way that chlorophyll is distributed among the micelles. This will be detailed in Results and discussion.

2.3. Spectroscopy

Absorption spectrometry was done in a Cary 5000 (SE) spectrophotometer (Varian). Circular dichroism (CD) spectrometry was done in an Aviv (Aviv Instruments) spectrophotometer.

Chl-*a* fluorescence was measured with SLM 8000TM-C spectrofluorometer (SLM-Aminco Rochester, NY). Self-absorption effects were avoided by using sufficiently low light absorbance (keeping the estimated total exciting light absorption or fluorescence self-absorption below 5%). In the high concentrations range we used special narrow cells (optical path 0.2 mm) positioned at 45° to both exciting and emission lights.

2.4. Fluorescence quenching measurements

For these measurements, Chl-*a* was first inserted into the micelles, at a much lower concentration than that of the carotenoids (mostly 0.5 μM), then the micelles were subjected to continuous fluorescence measurements during which a given carotenoid was added from its organic solution. For each experiment a proper control was performed by addition of a pure solvent alone. Chl-*a* was excited in the red region of its absorption, to avoid light absorption by the carotenoids.

The quenching extent is expressed in percent, as $100(1-F_c/F_b)$, where F_b is the basal (non-quenched) fluorescence level and F_c is the fluorescence level after addition of a carotenoid solution. In some cases it was necessary to correct for the quenching effect caused by the addition of a pure solvent. In this case the true quenching extent was calculated as $100(1-F_c/F_s)$, where F_s is the fluorescence level after addition of a pure solvent.

All determinations and experiments were carried out at room temperature.

3. Results and discussion

3.1. The micellar size

Our model system consisted of a solution mixture of Triton X-100 (*p*-(1,1,3,5-tetramethylbutyl) phenoxy polyoxy-ethylene glycol, with 9.5 oxyethylene units per molecule on the average),

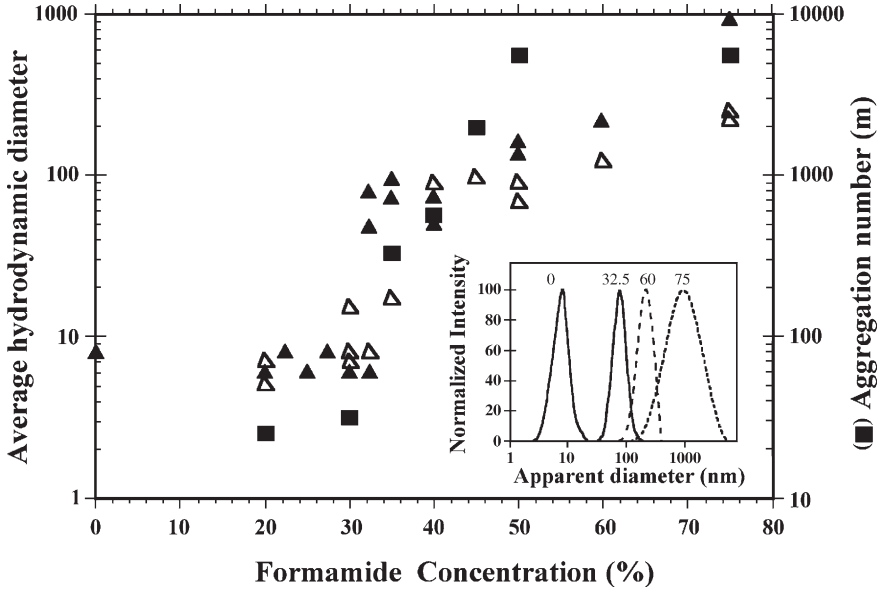

Fig. 1. Dependence of the micellar size on formamide concentrations. Main figure: apparent average diameter from QELS (left ordinate axis) and aggregation numbers (**m**) from Chl fluorescence self-quenching (right ordinate axis) as functions of FA concentration. ▲—average diameter for 0.2% TX-100 in water/FA. △—average diameter for 0.4% TX-100 in water/FA. ■—average aggregation number (**m**) for 0.4% TX-100 in water/FA. Insert: Apparent micelle diameter distribution for several chosen values of FA concentration (indicated as % at the top of each distribution curve) for 0.2% TX-100 in water/FA.

formamide and water. It was used to form micelles, with the rational to trap single chlorophyll molecules together with single carotenoid molecules in each micelle. For optimal conditions, it was necessary to know how these pigments are distributed among the micelles. This distribution depends on the relative pigment content and the number of micelles. The later is given by the ratio of the overall detergent concentration divided by the aggregation number (**m**). As a first step we measured the geometric size at different FA concentrations, using QELS.

From QELS measurements we obtained profiles of the size distribution at different concentrations of FA (Fig. 1, insert). From this and similar data it was possible to extract average micellar diameters, which are collected in the main Fig. 1 for two TX-100 concentrations (0.2 and 0.4%). The average micellar diameter increases enormously as a function of increasing FA concentrations, from 7−10 nm to eventually >1000 nm. Of special notice is the relatively sharp increase of the average diameter, at around 30–35% FA, from its lower value to about 100 nm.

For the aggregation number **m**, we used an approach based on the self-quenching of Chl-*a* fluorescence at high Chl-*a* concentration [21], and the manner in which Chl-*a* is distributed among the micelles. Fig. 2 shows plots of the intensity of Chl-*a* fluorescence as a function of its average concentration (in a range 0–30 μM), at various FA concentrations. Between 0 and 30% FA, these plots are nearly linear. Above 35% FA, noticeably between 40 and 50% FA, the range of linearity was limited to smaller Chl-*a* concentrations and at higher concentrations

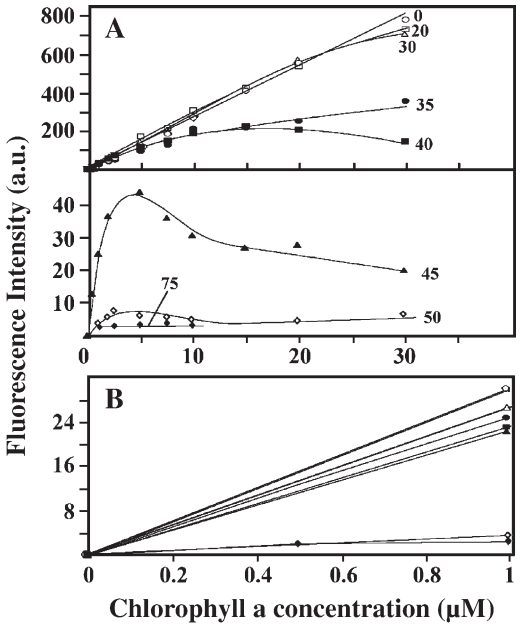

Fig. 2. Chl-*a* fluorescence intensity vs. concentration in TX-100 micelles, for different FA concentrations. Chl-*a* dissolved in pyridine was added in small portions to micelles made from 0.4% TX-100. Fluorescence was measured from a 0.2×10 mm cell, placed obliquely to the excitation beam (Excitation 610 nm; Emission wavelength 680 nm. Slits 16 and 4 nm, respectively). A—Top panel: data for 0–40% FA (–○– 0%, –□– 20%, –△– 30%, –●– 35%, –■– 40%); Bottom panel—data for 45–75% FA (–▲–45%, –◇–50%, –◆–75%); B—comparison of the initial slopes of the fluorescence curves in the range 0–1 μM for the different FA concentrations (symbols as above). Note the different fluorescence intensities in the three panels.

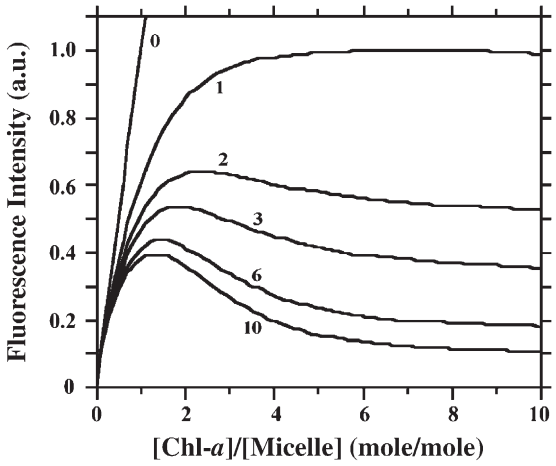

Fig. 3. Theoretical plots of the relative fluorescence intensity vs. the ratio [molar Chl-*a* concentration]/[molar micellar concentration]. The different curves correspond to various values of the Stern–Volmer parameter *b* (see Eqs. (2) and (3)).

the fluorescence tended to saturation and even decreased. At 75% FA the fluorescence was very low, achieving saturation at extremely low Chl-*a* concentration. These last effects are explained by a distribution pattern in which the majority of micelles contain a number of Chl-*a* molecules and self-concentration quenching comes to play[1].

Since the plots in Fig. 2 reflect different distribution patterns of Chl-*a* for different FA concentration, it is possible in principle to obtain from them the **m** values, which govern the distribution. Using a simplified analysis (cf. Appendix A) we obtained the following formula for the fluorescence as a function of Chl-*a* concentration:

$$F \propto \Sigma_k \frac{x^k}{[1+b(k-1)](k-1)!} e^{-x} \qquad (1)$$

where x represents the ratio of concentrations [Chl-*a*]/[micelle]; b is a parameter equal to the ratio between the quenching rate constant and the sum of all other rate constants for fluorescence and radiationless transition, divided by the product of Avogadro number and the micellar volume. The converging infinite sum is performed over the running index k (=0, 1, 2..., etc.). In practice, the sum was truncated at k=21, which was sufficiently precise for the used range of x.

Fig. 3 shows a selection of normalized theoretical plots for F vs. x according to the above equation, calculated for various chosen values of b. The plots become nearly insensitive to changes in b for b>10. It is seen that the shapes of the series of curves in Fig. 3 are similar in general to the shapes of the series of experimental curves in Fig. 2. We explored the possibility to

[1] One should note that the effect of FA is dual. According to the theoretical model, the initial slope in the linear range, represents the maximum Chl-*a* fluorescence quantum yield (i.e. in the absence of self-quenching) and only the deviation from a linear dependence represents the self-quenching effect. In our case, an increase of FA beyond about 30% changed also the initial slope, reflecting a change in the (maximal) quantum yield of Chl-*a* fluorescence. This second influence of FA represents a "solvent" effect (i.e. that of the molecular environment as such). In particular, at 75% FA the solvent effect is very strong to cause the fluorescence to remain very low.

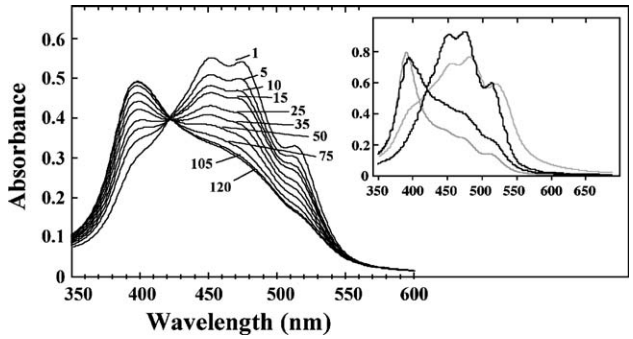

Fig. 4. Absorption spectra of zeaxanthin in TX-100 micelles in the transition from a J-type ("head to tail") dimer form to a H-type ("card pack") form. Micelles were made from 0.25% TX-100 and 40% FA. The time (in minutes) elapsing from the insertion of zeaxanthin into the micelles is indicated near each spectral curve. Zeaxanthin concentration ca. 5 μM. Insert: spectra of zeaxanthin in micelles compared to those in aqueous acetone. Black curve with the right peak—zeaxanthin added from its tetrahydrofuran (THF) solution to micelles and measured immediately; black curve with the left peak—zeaxanthin added from its pyridine solution to micelles and measured after stabilization (THF slowed the transition, allowing precise measurement of the initial spectrum). Grey curve with the right peak—zeaxanthin in 50% water aqueous acetone (enriched in J-type); grey curve with the left peak—zeaxanthin in 70% water aqueous acetone (enriched in H-type). Zeaxanthin concentration in the micelles ca. 8 μM. The spectra in acetone were normalized to approximately match those in the micelles.

approximately superimpose a chosen experimental plot with a theoretical one (by separate scaling in the horizontal and vertical directions). Although this is somewhat subjective, it yielded surprisingly a close match. For such two matched curves the abscissa values in the first one are expressed in terms of Chl-*a* concentration and in the second one in terms of the ratio [Chl-*a*]/[micelles]. The equivalence of the two allows one to calculate the micellar concentration for each case and hence the aggregation number **m**. For specific examples see Appendix B.

The results of this analysis for the aggregation number, **m**, vs. FA concentration is brought in Fig. 1 also (closed squares). The two independent sets of data, QELS and Chl-*a* self-quenching analysis, lead to the same conclusion—that the micellar volume increases enormously as the FA concentration increases from about 30% on. Both the apparent hydrodynamic diameter and aggregation number change in parallel and the range of the effect is very large, comprising at least two orders of magnitude. Also, both parameters exhibit a similar sharp increase at the same FA concentration range (about 30–35%). This agreement gives confidence to both types of measurements. In addition, the c.m.c. values, reflecting in some way the change in the micellar size, also varied considerably with FA concentration (3 c.m.c. determinations were: 0.09, 1.3 and 3.1 mM for 0, 40, and 75% FA, respectively, in agreement with [33] for 0% FA and [25] for 75% FA).

3.2. Spectroscopy of the carotenoids in the micelles—spectral changes and kinetics

When added to the micellar system zeaxanthin exhibited time dependent spectral changes. The initial spectrum differed from the spectrum in the organic solvent and contained an additional band at a longer wavelength (ca. 520 nm). This long-wavelength absorbing form was slowly converted to a short-wavelength absorbing form, with a UV prominent band at about 350 nm (Fig. 4). The dimethoxy derivative of zeaxanthin in micelles exhibited only the initial spectral type (cf. Table 1), which was completely stable.

These unexpected spectral changes can be compared to literature reports for xanthophylls in aqueous organic solvents [34–37]. In this case an extensive change of the UV/visible absorption spectrum occurs, mostly with a loss of the characteristic absorption peaks in the visible range and formation of a new UV band. In the measured cases of lutein and zeaxanthin such changes were accompanied by characteristic circular dichroism (CD) spectra, which indicated the formation of aggregated forms [36,37]. In contrast, the diesterified forms of lutein and zeaxanthin behaved differently, preserving the visible spectral bands with a formation of an additional band at a longer wavelength [36,37]. The difference in the behavior between non-esterified and esterified derivatives was attributed to two types of dimers (or higher aggregates)—parallel or "card pack" (H-type) in the first case (with a UV band) and "head to tail" (J-type) in the second case (with a visible

Table 1
Spectral parameters (wavelength positions in nm and relative intensities) of J-type zeaxanthin aggregate, from the absorption and CD spectra of zeaxanthin and its OH substituted derivatives, in different environments

	Zea in aqueous acetone (49.37% water)[a]		Zea diacetate in aqueous ethanol (75% water)[b]		Zea dimethoxy in aqueous acetone (50% water)[c]		Zea in micelles[a]		Zea bound to PsbS[d]	
	λ	Intensity	λ	Intensity	λ	Intensity	λ	Intensity	λ	Intensity
Absorption spectrum	517 (p)	1	514 (p)	1	514 (p)	1	513 (p)	1	523 (p)	1
	481 (p)	1.3	474 (p)	1.6	478 (p)	1.53	476 (p)	1.5	480 (p)	1.13
	456 (p)	1.2	448 (p)	1.7	450 (p)	1.50	452 (p)	1.45	452 (p)	1.12
	428 (s)	0.9	423 (s)	1.2	430 (s)	1.3	428 (s)	0.96	425 (s)	1
CD spectrum	545 (p)	1	518 (p)	1	N.A.		516 (p)	1	536 (p)	1
	508 (p)	0.79	482 (p)	1.57			483 (p)	1.36	491 (p)	0.9
	475 (s)	0.13	459 (s)	0.71			457 (s)	0.35	467 (s)	0.7
	422 (t)	−1.2	416 (t)	−1.2			423 (t)	−0.62	380 (t)	−1

All spectral intensities are normalized to that at the longest wavelength peak. (p)—peak; (s)—shoulder; (t)—trough.
[a] This work—similar results were obtained in [39].
[b] From [36].
[c] This work.
[d] From [30].

band). The spectral features of the dimers (aggregates), compared to those of the monomers are generally attributed to excitonic interactions [38]. Recently, we observed the formation of a J-type zeaxanthin form in aqueous acetone, which exists in a rather narrow range of water concentration (cf. Table 1 and inserts to Figs. 4 and 7), as was also reported independently [39].

Comparison of the zeaxanthin initial spectrum obtained in the micellar system with those obtained with zeaxanthin and its derivatives in the aqueous acetone case (Table 1) indicates that in the micelles only a J-type aggregate is formed initially upon insertion of zeaxanthin. Ultimately it undergoes a transition to a H-type aggregate until equilibrium between the two forms is reached. The insert in Fig. 4 shows the initial and final spectra in micelles, under conditions in which the transition is largely frozen or accelerated, comparing them to the spectra in aqueous acetone with 50% and 70% water, where the predominate zeaxanthin forms are J and H types, respectively.

The kinetics of J–H transition in the micelles follows a first order law, as shown in Fig. 5. The series of spectra recording this transition (Fig. 4) exhibits a well-defined isosbestic point, which occurred in all of our experiments, under a variety of conditions. This "clean" spectral transition in micelles between the J and H-types indicates a linear reaction [40]. This and the first order kinetic law indicate a simple reaction between two interconvertible species. From this argument it is largely unlikely that consecutive reaction involving large aggregates takes place and the observed spectral changes presumably represent dimeric moieties. The overall spectrum must be a superposition of contributions from micelles that contain only dimers (in which the transition takes place) and some micelles that contain only a single monomer molecule with fixed monomer spectrum. From the changes in the spectrum the dimer concentration is appreciable and the zeaxanthin concentration in the form of a dimer must be roughly half, at least.

The experiment of Fig. 4 was carried out with micelles in 40% FA. The changes in the micellar size as a function of FA concentration, as shown in Fig. 1, have significant influence on the spectroscopy and kinetics. This is summarized, at a low resolution, in Table 2. One may conclude that the formation of J-type dimers and the transition to H-type dimers can occur only in the larger micelles, while in the smaller micelles the monomer form predominates.

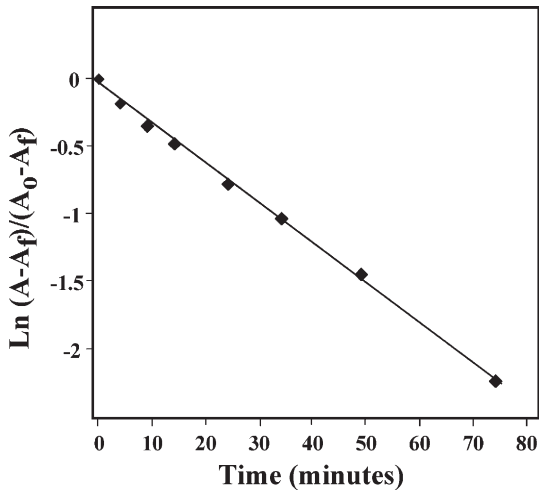

Fig. 5. A first-order kinetics plot for the conversion between the J-type and the H-type zeaxanthin aggregates in micelles. Data were taken from the experiment shown in Fig. 4. A is the momentary absorbance, A_0 is the initial absorbance and A_f is the (extrapolated) final absorbance. k (first order reaction constant)= 0.030 min^{-1}.

Table 2
The effect of FA concentration on the spectra of zeaxanthin in the micellar system

% FA	Initial spectral type [a]	Final spectral type [a]
10	All A	All A
20	All A	All A
30	All A	Some C
40	Mostly B	Mostly C
50	Mostly B	Mostly C

[a] Spectral types: A: monomeric-similar to that in an organic solvent; B: with the appearance of the peak at around 510–520 nm signifying the J-type dimer. C: with the peak at the UV signifying the H-type dimer alone.

The spectral transition shown in Fig. 4 was obtained at 5 μM zeaxanthin. In the various repeated experiments at different zeaxanthin concentrations (between 3 and 10 μM) for 0.2–0.4% TX-100 we always obtained similar profiles and extents of spectral changes. Using the **m** values from Fig. 1, it turns out that for the lowest zeaxanthin concentration the micelle concentration exceeds considerably that of zeaxanthin. In this case the calculated fraction of micelles containing two or more zeaxanthin molecules is very small (see Appendix C) hence also the expected fraction of possible dimeric forms. This implies that the simplistic view that zeaxanthin molecules are first distributed into the micelles as monomers and then transformed into dimeric forms cannot be correct. The presence of significant fraction of dimeric (or aggregated) forms in micelles, over a wide range of zeaxanthin concentrations, implies that prior to the entrance into the micelles a major fraction of zeaxanthin is already converted to dimeric or aggregated entities and as such are distributed randomly into the micelles. This explains why a major fraction of occupied micelles contain two (or more) combined monomeric entities. This conclusion makes sense, since the first event following the injection of the zeaxanthin from its pyridine solution to the micellar solution is its solubilization in the aqueous phase, in which it becomes aggregated.

The above spectral changes in micelles are unique to zeaxanthin. Fig. 6 shows that, in contrast to zeaxanthin, no spectral changes of lutein and neoxanthin occurred in micelles, although their aggregated forms exist in aqueous acetone [34,37]. Their spectra in micelles are sufficiently close to those in an organic solvent, representing essentially monomeric forms. β-carotene remains monomeric both in micelles and in aqueous acetone.

The behavior of violaxanthin in micelles, however, is more similar to that of zeaxanthin, showing two new peaks—a strong UV peak corresponding to the H-type dimer in micelles and a minor long wavelength peak corresponding to the J-type dimer (Fig. 6). However, this spectrum is obtained immediately upon violaxanthin insertion. If there is a transition between the two types it is too fast to be resolved.

Aggregated forms are characterized by the appearance of circular dichroism (CD). Upon insertion of zeaxanthin into the micelles an intense CD spectrum was indeed immediately

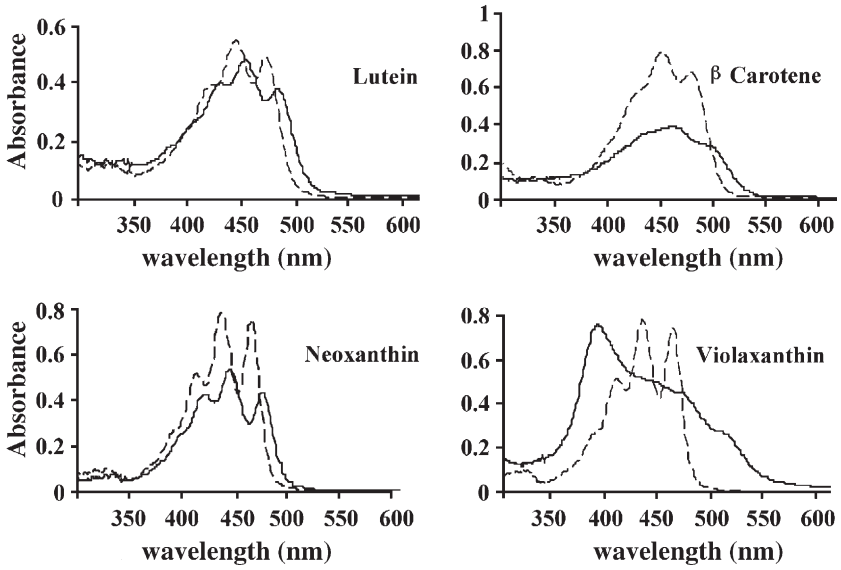

Fig. 6. Absorption spectra of lutein, neoxanthin, β-carotene and violaxanthin in TX-100 micelles (solid curves) and organic solvents (n-hexane for β-carotene and ethanol for the rest—dashed curves). The micellar solutions contained 0.2% TX-100 and 40% FA. The concentration of the carotenoids was approximately 4 μM.

observed, which underwent a transition to another CD spectrum, parallel to the change in the ordinary absorption spectrum (Fig. 7). These CD spectra are similar to those of zeaxanthine in the aqueous acetone case, under conditions where the J- and H-forms are obtained (Fig. 7, insert). Similarly to zeaxanthin, violaxanthin had also a strong CD signal in the micelles (Fig. 7). However, none of the other caroteneoids (β-carotene, neoxanthin, lutein) gave any noticeable CD signal in micelles, in agreement with the absorption spectra exhibited by these compounds (Fig. 6).

3.3. Chl-a form in the micelles

In contrast to the tendency of zeaxanthin and violaxanthin to dimerize, Chl-*a* did not exhibit any changes in its normalized absorption spectrum by varying its concentrations over a wide range at various FA concentrations, including conditions under which fluorescence self-quenching was prominent (data not shown). Likewise, no CD signal was observed and the normalized fluorescence emission spectrum remained unchanged.

This behavior stands in contrast to that of bacteriochlorophyll a (BChl-*a*), which tends to form ground-state dimers and larger aggregates [25,41], marked by changes in the absorption spectrum. The micellar size itself was sensitive to the presence of BChl-*a* [42], which was attributed to the tendency of BChl-*a* to aggregate and connect several micelles into one unit. This particular effect was absent here as Chl-*a* tendency for a similar dimerization or aggregation is weak.

3.4. Chl-a fluorescence quenching by the carotenoids—a comparison

The effect of an added carotenoid on Chl-*a* fluorescence was measured by continuously monitoring the fluorescence intensity of Chl-*a*, dissolved in micelles, and observing the changes that occur upon the addition of a specified carotenoid. For optimal conditions, the chlorophyll concentration should be much smaller than that of the micelles, as well as than that of the carotenoid. This ensures practically that any given micelle contains either no or only a single chlorophyll molecule. It also ensures that the

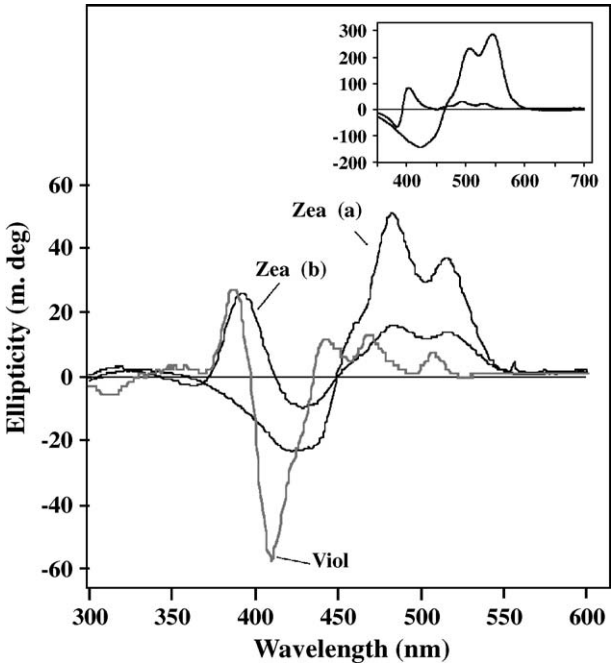

Fig. 7. CD spectra of zeaxanthin and violaxanthin. Zea (a)—zeaxanthin in micelles, added from its solution in THF to slow down the transition and measured immediately (cf. Legend to Fig. 4). Zea (b)—zeaxanthin in micelles, added from its solution in pyridine and measured after equilibration. Viol-violaxanthin in micelles. Concentration of the xanthophylls ca. 8 μM. Micellar composition: 0.4% TX-100 and 40% FA. Insert: CD spectra of zeaxanthin dissolved in aqueous acetone. Spectrum with the positive peak at right—zeaxanthin in 50% water aqueous acetone (enriched in J-type aggregate); spectrum with the positive peak at left—zeaxanthin in 70% water (enriched in H-type aggregate).

distribution pattern of molecules of another pigment among the sub-set of micelles that already contain a Chl-*a* molecule is the same as among the entire micelle population. Under these conditions there is no possibility for Chl-*a* self-interaction.

Because of its ready availability and known quenching ability in solution [22], β-carotene served as a convenient model compound, to test the behavior of the model system in general and as a standard for comparison to the other carotenoids. Fig. 8 shows raw data for the effect of β-carotene on Chl-*a* fluorescence in micelles containing different proportion of FA. For low FA concentrations, up to about 30%, no or very little quenching was noticed. There was an abrupt jump to maximal quenching at 40% FA, extending to 50%. At 70% the quenching became smaller but still significant.

This experiment draws a parallel between the conditions shown for Chl-*a* self-quenching related to the micellar size (Fig. 1) and the quenching by β-carotene. Accordingly, the increase of FA concentration causes a large increase in the micellar size, with a jump in size at around 35% FA. Below this FA concentration the micellar size is small, the number of micelles in a unit volume is relatively large and the distribution of Chl-*a* and β-carotene is such that the probability that both will reside in the same micelle is very small. Above 35% the size increases several fold, the number of micelles decreases correspondingly and the probability that both pigments will be distributed into one micelle becomes sufficiently large. The strong FA solvent quenching effect at still higher FA concentration (Fig. 2) is probably the reason that the additional measured quenching effect of β-carotene decreases. This sets an optimal FA concentration around 40–50% for the effect of β-carotene. A quantitative support for the above argument will be given below.

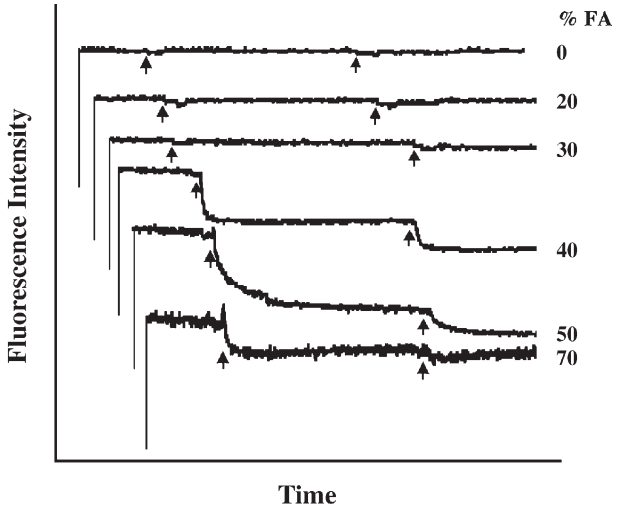

Fig. 8. Raw data for Chl-*a* fluorescence quenching by β-carotene in micelles at different FA concentrations. Chl-*a* (0.5 μM) was inserted into micelles (0.4% TX-100 and variable amounts of FA in water, as indicated). β-carotene was added from its pyridine solution at two time points, as marked by the arrows, to final concentrations 4 and 8 μM, respectively. Chl-*a* fluorescence was excited by 640 nm light and measured at 680 nm. A full fluorescence emission spectrum was also taken (not shown) showing the characteristic fluorescence spectrum of Chl-*a*. Full time scale for the experiment varied between curves, around approximately 2 min.

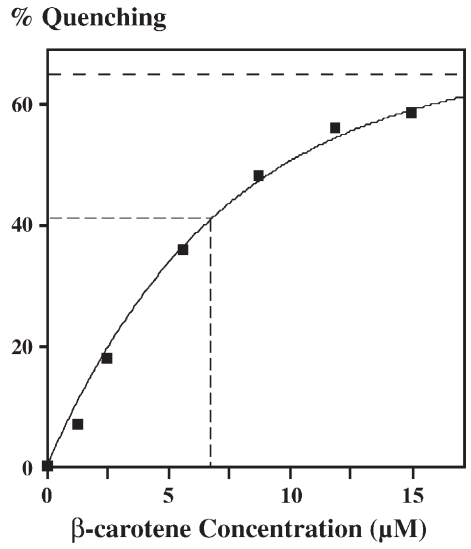

Fig. 9. β-carotene concentration dependence of chlorophyll a fluorescence quenching in micelles. Experimental conditions were similar to that of Fig. 8 with FA concentration 40%. The extrapolated maximum quenching and the point where the quenching is $(1-1/e)$ of the maximum are indicated by the dashed lines.

In these experiments and in most of the following ones, β-carotene and other carotenoids were added from their solution in pyridine. We noticed that pyridine also induced some quenching effect by itself, which was particularly strong for micelles made from 0.2% triton X-100. This required corrections for the pure solvent effect. Fortunately, in micelles at a concentration of 0.4% TX-100 (as used in Fig. 8) this effect was quite small and could be neglected.[2]

As will be documented below, of all the investigated carotenoids only β-carotene and zeaxanthin were strong quenchers of Chl-*a* fluorescence. The comparison of the quenching abilities was based on the carotenoid concentration dependence of the quenching. β-carotene served as a convenient model compound to investigate this dependence, which is shown in Fig. 9. Accordingly, the extent of quenching is approximately linear at sufficiently small concentrations, but as the concentration increases the quenching curve gradually inclines and tends towards saturation. Obviously, the linear range reflects the increased probability that a single quencher molecule occupies any given micelle (including the ones which already contain Chl-*a* molecule). The tendency to saturation is related to the extrapolated situation where a sufficient number of quencher molecules occupy each micelle. According to the analysis of the data of Fig. 9, brought in Fig. 10, the difference between the extent of quenching at any point and the maximum quenching (Qs) line fits nicely a decreasing exponential function. This equation results from the model of

[2] Tetrahydrofuran and particularly ethyl acetate by themselves affected the fluorescence of Chl-*a* in 0.2% TX-100 micelles to a much lesser degree. Still, pyridine was preferred as a solvent, resulting in the best reproducibility, although essentially all results were similar. Solvents such as benzene and chloroform did not enter at all into the micelles and their β-carotene solutions were inactive towards chlorophyll fluorescence. A careful observation showed indeed that they formed unmixed separate phases.

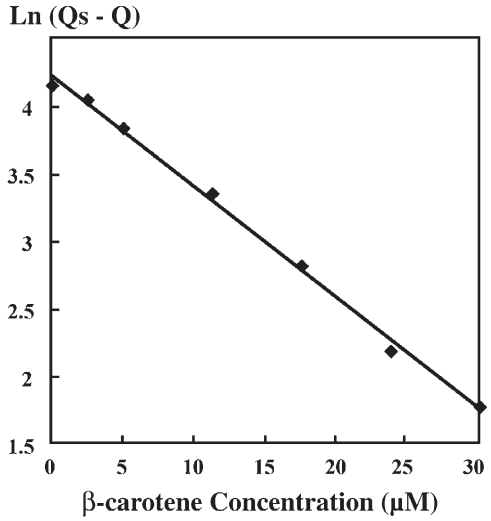

Fig. 10. Plot of Ln (Qs–Q) vs. β-carotene concentration. Data were taken from the experiment of Fig. 9.

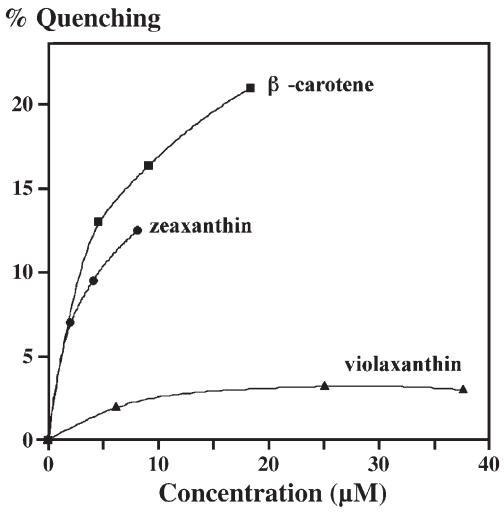

Fig. 11. Concentration dependence of the quenching of Chlorophyll a fluorescence exerted by β-carotene, zeaxanthin and violaxanthin. Quenching measurements were made successively with the same batch of micelles (0.4% TX-100 and 40% FA in water). Chl-*a* concentration was 0.5 μM.

random Poisson distribution of the quencher molecules among the micelles, but with the additional assumption that a single quencher molecule exerts already maximum quenching effect. In this case the resulting equation is: $Q = Qs\ (1 - \exp\ \{-[\text{quencher}]/[\text{micelles}]\})$, where the square brackets indicate the molar concentrations. From this equation it follows that the point where the quenching is $(1 - 1/e)$ of the maximum corresponds to a quencher concentration equal to the micellar concentration. This point corresponds in Fig. 9 to an overall concentration of the quencher of 6.8 μM. Calculation of the micellar concentration under these conditions, from the molar concentration of TX-100 and the aggregation number **m**, using Fig. 1, gives a figure of 5.5 μM for the micelle concentration. These two numbers deviate by only about 20%, which is quite satisfactory, considering that **m** may broadly vary between different micelle preparations and that the precision in the β-carotene amount is in the order of 10%. This also explains the result of Fig. 8, since at small FA concentrations below 30%, the aggregation number is about 20 times less (Fig. 1), hence the micelle concentration is 20 times higher resulting in negligible quenching.

There is, however, one problem with this model, which neglects the effect of additional quencher molecules that occupy a single micelle. The quenching is expected to increase by a mass action law, e.g., according to the Stern–Volmer model, so that the quenching should tend to 100% at sufficiently high carotenoid concentrations. This is clearly neither the case in Fig. 9 nor in all other experiments, with zeaxanthin as well. In the case of Fig. 9 the quenching tended to a limit of about 65% (found from the exponential extrapolation). At the moment we can provide only a tentative guess to this dilemma. It is possible that Chl-*a* and one of the carotenoids forms a close-distance ground-state associate or complex, in which the carotenoid moiety acts as a quencher. The quenching in this case is not "dynamic" (i.e., involving collisions of the quencher with the excited state substrate), but rather "static". Possibly the micellar medium constrains such associate into a configuration, which is not optimal for maximum quenching, or that there is a distribution of possible orientations and distances of the two partners resulting in an overall quenching smaller than the maximum. Such complex may be sufficiently bulky to prevent other carotenoid molecules to reach a proper interaction distance or orientation from the Chl-*a* molecule, as to exert a mass action.

The maximum quenching varied in different experiments, roughly between about 30–60% (a few exceptions gave lower values). There was also some variability (of the order of 20%) in the concentration range for the concentration dependence, due to possible variability in **m**. Part of this variability could be related to the sensitivity of the micellar parameters to the details of their preparations as well as the elapsing time until the start of the experiment, which could not be controlled properly. Important, however, is the fact that for any single batch of micelles the results were always much more consistent. Hence, for comparing the effect of the various carotenoids, only results related to the same micelle preparation were used.

Having obtained the above data with β-carotene, we obtained the quenching abilities of zeaxanthin, violaxanthin, lutein and neoxanthin towards excited Chl-*a*, in comparison with β-carotene. Three representative results from different experiments are shown. Fig. 11 shows an example for the concentration dependence of the quenching by β-carotene, zeaxanthin and violaxanthin. In Table 3 we show results of 4 typical different experiments for the ratio

Table 3
Specific quenching capacity (initial slope of the quenching vs. overall quencher concentration in the micellar solution) for β-carotene, zeaxanthin and violaxanthin—representations of 4 different experiments

Compound	Quenching (%)/Concentration (μM)			
β-carotene	1.01	1.25	1.14	0.3
Zeaxanthin	1.42	1.11	1.50	0.57
Violaxanthin	0.08	0.17	0.13	0.07

Micelles were made as described. Triton X-100 concentration was 0.2% for the left two columns and 0.4% for the two right columns. FA concentration was 40%.

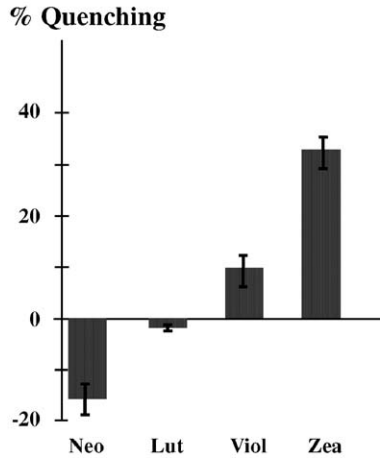

Fig. 12. Comparison of the effects of neoxanthin (NEO), lutein (LUT), violaxanthin (VIO) and zeaxanthin (ZEA) on chlorophyll a fluorescence. Micelles were made as in Fig. 11. Chl-*a* concentration was 0.1 μM. Concentration of the xanthophylls was 5 μM.

quenching/concentration (i.e., the initial slope of the quenching concentration curve) obtained for these compounds in a concentration range where the quenching is linear with the concentration. This representation exemplifies also the type of variability obtained between different batches of micelles. In Fig. 12 we compare the saturation values of the quenching of all the above compounds. Overall, the relative quenching abilities stand in the order zeaxanthin≈β-carotene>>violaxanthin. Only β-carotene and zeaxanthin were good quenchers of Chl-*a* fluorescence. Violaxanthin was a much weaker quencher compared to zeaxanthin. Lutein and neoxanthin rather enhanced the fluorescence. Similar results were obtained for TX-100 micelles with 75% FA, reported much earlier in [26].

The zeaxanthin quenching ability must evidently be related to the J-type dimer, formed immediately upon the addition of zeaxanthin. Taking into account the kinetics of the conversion to the H-type form, the quenching was probed at different times when zeaxanthin was either mostly a J-type or H-type dimer, resulting in even higher quenching for the H-type (results not shown). The results for violaxanthin are related essentially to the mixture of J and H-types dimeric form, as present in the micelles.

4. Concluding discussion

The micellar size and its dependence on the composition of the micellar solution are important and relevant for probing pigment interactions, as they determine the distribution pattern of the pigments in the micelles. This was probably overlooked by a previous study of carotenoids and chlorophyll in a model system made of liposomes [43]. In the present work FA concentration was a factor to establish the correct conditions for pigment interactions: as it increased the micelles became bigger, their number decreased, and vice versa. In addition, it is quite probable that the micellar volume, as such, is important, in order to be able to conveniently accommodate two pigment molecules at least. It turned out that for the range of TX-100 concentration and overall pigment concentrations used here (in the μM range), an optimal micellar size is obtained at around 40−50% FA. In our experiments diverse phenomena, such as concentration self-quenching of chlorophyll fluorescence, the formation and transition between the dimeric forms of zeaxanthin and the quenching of chlorophyll fluorescence by β-carotene and zeaxanthin had similar FA concentration dependence. This parallelism validates the results of the QELS measurements also to the case where the micelles contain pigments.

Comparing all the investigated carotenoids, only zeaxanthin and violaxanthin formed dimers in micelles. Zeaxanthin had the strongest tendency to form the J-type aggregate, both in micelles and in aqueous acetone at around 50% water, where the concentration of the J-type aggregate was appreciable. In comparison to zeaxanthin, only violaxanthin was somewhat similar as it formed in micelles an equilibrium mixture of H and J-types, but the former was predominating, showing that the J-type dimer of violaxanthin is less stable. In contrast, all the other xanthophylls did not form aggregates at all in micelles; in aqueous acetone they formed mainly the H-type aggregate and the J-type was hardly discernible even at optimal conditions. This makes zeaxanthin and to lesser extent violaxanthin unique species. The differential behavior of zeaxanthin and violaxanthin contra other carotenoids with respect to their tendency to dimerize is interesting and could play a part in their function in the photosynthetic apparatus.

Aspinal-O'Dea et al. [30] reported binding of zeaxanthin to isolated PsbS light-harvesting complex of the chloroplasts photosynthetic machinery. This binding changed the original spectrum of zeaxanthin in such a way that a new band appeared in the long-wavelength side, peaking at about 523 nm. At the same time an intense CD spectrum appeared. The absorption and CD spectra resemble the spectra that were obtained in aqueous acetone and in micelles for the J-type zeaxanthin dimer (Table 1). This finding is interesting as the PsbS protein could be the site of zeaxanthin dependent NPQ [8]. One may conclude that binding of zeaxanthin to PsbS results in zeaxanthin J-type dimer formation. Whether two zeaxanthin molecules bind and form a dimeric structure within a single protein molecule, or two protein molecules, each with one bound zeaxanthin molecule, interact and form a dimer, is too early to decide. Also, one has to determine whether this binding is a specific one or represents only a physical adsorption.

Similar absorbance changes at around 538 nm were noticed also in thylakoid membranes under the transition to a "non photochemical quenching" state [29,35] and could be assigned to the formation of zeaxanthin J-dimer, considering that the shift to longer wavelengths could be due to the special in-vivo environment.

The above in-vivo spectral changes encourage us to believe that dimeric forms of zeaxanthin could indeed be relevant to the understanding of the interaction between Chl-*a* and the xanthophylls in-vivo. Our results on the differential quenching are consistent with the view that dimeric zeaxanthin can form a quenching center for the LHC-II excitation. Unfortunately, the micellar system is not entirely conclusive in comparing the quenching capacities of the xanthophylls, since actually different forms are compared (J or H-types of zeaxanthin vs. a mixture of dimeric types for violaxanthin and monomeric types for the other xanthophylls). There is no sure answer for the quenching capacities of

monomeric zeaxanthin and violaxanthin. Regarding monomeric zeaxanthin, at least, it is quite reasonable that it may be also a strong quencher as β-carotene, based on the similarity of structures.

In spite of the above reservations, let us assume that indeed dimeric forms of zeaxanthin are produced under NPQ conditions in LHC-II, serving as quenching centers. The transition to NPQ conditions must involve a process that occurs over a scale of supramolecular organization of LHC-II in the photosynthetic membrane [44]. Over this scale, one may imagine that two molecules of zeaxanthin from two LHC-II units come together to form a dimer and act as a quenching center for the entire complex. As mentioned above, this view is in harmony with the observation that conformational and corresponding spectroscopic changes accompany this process [7,44] and with the evidence that speaks for the specific participation of the PsbS protein in NPQ [8], which is present in small amounts and thus its effect must be expressed on a scale of a supramolecular structure.

There is an apparent discrepancy between the extrapolated maximum quenching achieved in the micellar system (mostly more or less around 30–50%) and the in-vivo system under NPQ conditions (around 80–90%). As said above, the micellar system is not perfect in that the mutual geometry of zeaxanthin and chlorophyll is not well defined. The two may be trapped in the micelles in a non-optimal geometry or in a variety of distances and orientations, leading to various degrees of interaction and hence of quenching, with an overall smaller quenching than the maximum possible. In the in-vivo case the geometry is probably well defined leading to strong interaction and considerable quenching. This is a point where the model system should be improved in a future work.

One may note a recent paper, which expresses a contrasting view by showing a detailed crystal structure of trimeric LHC-II [45]. The structure shows the positioning of four carotenoids in each monomeric unit, including that of violaxanthin. The authors tend to conclude that NPQ occurs by simple replacement of violaxanthin with zeaxanthin, still however with no solid proof and without considering the changes brought about on the supramolecular scale.

In conclusion, we have shown in the model system differential quenching abilities of the carotenoids, which may fit certain theories of NPQ mechanism. It is hoped that these results will promote further research into these possibilities.

Acknowledgements

We wish to thank Prof. Hugo Scheer, University of Munich, for critical reading of the manuscript and helpful comments, to Ms. Ilona Eizen and Ms. Olga Furman for technical assistance. Thanks are due to Dr. Ellen Wachtel, of the Chemical Research Support of the Weizmann Institute for her help in the QELS measurements.

Appendix A. Derivation of the fluorescence intensity as a function of the concentration ratio [Chl-a]/[micelle]

As a first approximation to the analysis of Fig. 2, we use a simplified model, which assumes: (1) A single micellar size, instead of a distribution, (2) Poisson distribution of the Chl-a molecules in the micelles and (3) Stern–Volmer law equation for the quenching in each micelle. The analysis will lead to the micelle concentration and **m** will be simply calculated as the ratio of concentrations [TX-100]/[micelle] (assuming negligible detergent in solution outside of the micelles).

Assuming Poisson distribution, the relative concentration, c_k, of a sub-population of micelles containing k Chl-*a* molecules, for a given molar concentration ratio, x, of Chl-*a* to the micelles is:

$$c_k = \frac{x^k}{k!}e^{-x} \tag{1}$$

For a micelle where one of the Chl-*a* molecules is excited, the concentration of ground state Chl-*a* molecules is taken to be equal to $(k-1)$ divided by the product of Avogadro number and the micellar volume. Hence the fluorescence yield, ϕ_k, from such micelles, using the Stern–Volmer law is:

$$\phi_k \propto \frac{1}{1+b(k-1)} \tag{2}$$

where b is a parameter equal to the ratio between the quenching rate constant and the sum of all rate constants for fluorescence and radiationless transition, divided by the product of Avogadro number and the micellar volume. For the linear range of light absorption vs. concentration, the light absorption into micelles with k Chl-*a* molecules is weighted by k. It follows therefore that the total fluorescence intensity is given by summing over all micelles:

$$F \propto \Sigma k\phi_k c_k = \Sigma \frac{x^k}{[1+b(k-1)](k-1)!}e^{-x} \tag{3}$$

Appendix B. Specific examples of the fit between the experimental (Fig. 2) and theoretical (Fig. 3) plots of Chl-a self-quenching in the micelles and calculation of m

One example for such fit is the case of micelles with 45% FA. It was possible to approximately fit most of the corresponding curve of Chl-*a* fluorescence vs. concentration (Fig. 2A, bottom) to the theoretical curve (Fig. 3) with $b=6$. This fit made a correspondence of 30 μM Chl-*a* with a concentration ratio [Chl-*a*]/[micelle]=9. The micelle concentration is therefore 30/9=3.3 μM. The TX-100 concentration was 0.4% (=6540 μM) and therefore **m**=6540/3.3=1980. Using the same value of b (=6), a fit was also made to the curve of Chl-*a* fluorescence vs. concentration for 30% FA. In this case 30 μM Chl-*a* corresponded to [Chl-*a*]/[micelle]=0.16, so that [micelle]=187 μM and therefore **m**=6540/187=35. In this procedure, after adjustment to a certain b value and evaluation of **m**, a second iteration was carried out, taking into account that b is inversely proportional to the micellar volume, which presumably is nearly proportional to **m** (assuming a constant density of monomer packing). The choice of a new b value for a theoretical curve resulted in a new value of **m**. Usually two iterations sufficed to achieve a satisfactory convergence of **m**.

Appendix C. Calculation of the probability of micelle occupation with two or more pigment molecules, under the experimental conditions related to Fig. 4, assuming random distribution of monomeric entities

From Appendix A, the probability that a micelle contains k pigment is: $(k!)^{-1}x^k \exp(-x)$, where x is the average occupation number, i.e., [pigment]/[micelle]. Therefore, the probability of micelle occupation by two or more pigment molecules is: $p_{\geq 2} = 1-(1+x)\exp(-x)$. In most of our experiments, the range of zeaxanthin concentration was such that x varied between about 0.3 to about 6, by varying also the concentrations of TX-100 (between 0.2 and 0.4%) and FA (between 40 and 50%), using the data of Fig. 1. For the lower range of x, $p_{\geq 2}$ is quite negligible (=approx. 0.04, 0.06 and 0.09 for $x=0.3$, 0.4 and 0.5, respectively. These small numbers stand in contrast to the appreciable dimer concentrations, expressed in our experiments, in the entire x range.

References

[1] P. Horton, A.V. Ruban, R.G. Walters, Regulation of light harvesting in green plants, Annu. Rev. Plant Physiol. Plant Mol. Biol. 47 (1996) 655–684.

[2] P. Horton, A.V. Ruban, M. Wentworth, Allosteric regulation of the light-harvesting system of photosystem II, Philos. Trans. R. Soc. Lond., B Biol. Sci. 355 (2000) 1361–1370.

[3] T.G. Owens, Processing of excitation energy by antenna pigments, in: N.R. Baker (Ed.), Photosynthesis and the Environment, Kluwer Academic Publishers, Dordrecht, 1996, pp. 1–24.

[4] B. Demmig-Adams, Carotenoids and photoprotection in plants: a role for the xanthophyll zeaxanthin, Biochim. Biophys. Acta 1020 (1990) 1–24.

[5] A.M. Gilmore, Govindjee, How higher plants respond to excess light: energy dissipation in photosystem II, in: G.S. Singhal, G. Renger, S.K. Sopory, K.-D. Irrgang, Govindjee (Eds.), Concepts in Photobiology: Photosynthesis and Photomorphogenesis, Narosa Publishing House, New Delhi, 1999, pp. 513–548.

[6] Govindjee, M.J. Seufferheld, Non-photochemical quenching of chlorophyll a fluorescence: early history and characterization of two xanthophyll-cycle mutants of *Chlamydomonas reinhardtii*, Funct. Plant Biol. 29 (2002) 1141–1155.

[7] A.V. Ruban, D. Rees, A.A. Pascal, P. Horton, Mechanism of ΔpH-dependent dissipation of absorbed excitation-energy by photosynthetic membranes II. The relationship between LHCII aggregation in vitro and qE in isolated thylakoids, Biochim. Biophys. Acta 1102 (1992) 39–44.

[8] K.K. Niyogi, X.P. Li, V. Rosenberg, H.S. Jung, Is PsbS the site of non-photochemical quenching in photosynthesis? J. Exp. Bot. 56 (2005) 375–382.

[9] N. Adir, H. Zer, S. Shochat, I. Ohad, Photoinhibition—A historical perspective, Photosynth. Res. 76 (2003) 343–370.

[10] G.H. Krause, E. Weis, Chlorophyll fluorescence and photosynthesis—The basics, Annu. Rev. Plant Physiol. Plant Mol. Biol. 42 (1991) 313–349.

[11] T.G. Owens, Excitation energy transfer between chlorophylls and carotenoids. A proposed molecular mechanism for non-photochemical quenching, in: N.R. Baker, J.R. Bowyer (Eds.), Photoinhibition of Photosynthesis, Bios Scientific Publishers, Oxford, 1994, pp. 95–109, chapter 5.

[12] H.A. Frank, A. Cua, V. Chynwat, A. Young, D. Gosztola, M.R. Wasielewski, Photophysics of the carotenoids associated with the xanthophyll cycle in photosynthesis, Photosynth. Res. 41 (1994) 389–395.

[13] T. Polivka, Direct observation of the (forbidden) S1 state in carotenoids, Proc. Natl. Acad. Sci. U. S. A. 96 (1999) 4914–4928.

[14] H.A. Frank, J.A. Bautista, J.S. Josue, A.J. Young, Mechanism of nonphotochemical quenching in green plants: energies of the lowest excited singlet states of violaxanthin and zeaxanthin, Biochemistry 39 (2000) 2831–2837.

[15] T. Polivka, D. Zigmantas, V. Sundstrom, E. Formaggio, G. Cinque, R. Bassi, Carotenoid S-1 state in a recombinant light-harvesting complex of photosystem II, Biochemistry 41 (2002) 439–450.

[16] H.A. Frank, S.K. Das, J.A. Bautista, D. Bruce, M.R. Vasiel'ev, M. Crimi, R. Croce, R. Bassi, Photochemical properties of xanthophylls in the recombinant photosystem II antenna complex, CP 26, Biochemistry 40 (2001) 1220–1225.

[17] P. Horton, A.V. Ruban, D. Rees, A.A. Pascal, G. Noctor, A.J. Young, Control of the light-harvesting function of chloroplast membranes by aggregation of the LHC II chlorophyll protein complex, FEBS Lett. 292 (1991) 1–4.

[18] A. Dreuw, G.R. Fleming, M. Head-Gordon, Charge-transfer state as a possible signature of a zeaxanthin-chlorophyll dimer in the non-photochemical quenching process in green plants, J. Phys. Chem., B 107 (2003) 6500–6503.

[19] A. Dreuw, G.R. Fleming, M. Head-Gordon, Chlorophyll fluorescence quenching by xanthophylls, Phys. Chem. Chem. Phys. 5 (2003) 3247–3256.

[20] N.E. Holt, D. Zigmantas, L. Valkunas, X.P. Li, K.K. Niyogi, G.R. Fleming, Carotenoid cation formation and the regulation of photosynthetic light harvesting, Science 307 (2005) 433–436.

[21] G.S. Beddard, G. Porter, Concentration quenching in chlorophyll, Nature 260 (1976) 366–367.

[22] G.S. Beddard, R.S. Davidson, K.R. Trethewey, Quenching of chlorophyll by β-carotene, Nature (Lond.) 267 (1977) 373–374.

[23] D.M. Gazdaru, B. Iorga, P.F. Balan, Quenching of chlorophyll a fluorescence by beta-carotene, Photosynthesis: mechanisms and effects, Proceedings of the International Congress on Photosynthesis, 11th, Budapest, Aug. 17–22, 1998, vol. 1, 1998, pp. 483–486.

[24] R.M. Hermant, P.A. Liddell, S. Lin, R.G. Alden, H.K. Kang, A.L. Moore, T.A. Moore, D. Gust, Mimicking carotenoid quenching of chlorophyll fluorescence, J. Am. Chem. Soc. 115 (1993) 2080–2081.

[25] V. Rosenbach-Belkin, P. Braun, P. Kovatch, A. Schertz, Optical absorption and circular dichroism of bacteriochlorophyll oligomers in triton x-100 and in light-harvesting complex B850—A comparative study, in: H. Scheer, S. Schneider (Eds.), Photosynthetic Light Harvesting Systems, Walter de Gruyter, Berlin, NY, 1988, pp. 323–337.

[26] S. Avital, S. Malkin, Quenching of chlorophyll fluorescence by carotenoids in micellar model system, in: J. Garab (Ed.), XI International Conference on Photosynthesis, Budapest, Kluwer, Dordrecht, 1998, pp. 477–482.

[27] S. Avital. Quenching of chlorophyll fluorescence by carotenoids in a micellar model system, Ph.D. thesis, The Feinberg school of the Weizmann Institute of Science, Rehovot, Israel. (2002) 88.

[28] A.V. Ruban, A.A. Pascal, B. Robert, P. Horton, Configuration and dynamics of xanthophylls in light-harvesting antennae of higher plants—Spectroscopic analysis of isolated light-harvesting complex of photosystem II and thylakoid membranes, J. Biol. Chem. 276 (2001) 24862–24870.

[29] A.V. Ruban, A.A. Pascal, B. Robert, P. Horton, Activation of zeaxanthin is an obligatory event in the regulation of photosynthetic light harvesting, J. Biol. Chem. 277 (2002) 7785–7789.

[30] M. Aspinall-O'Dea, M. Wentworth, A.A. Pascal, B. Robert, A.V. Ruban, P. Horton, In vitro reconstitution of the activated zeaxanthin state associated with energy dissipation in plants, Proc. Natl. Acad. Sci. U. S. A. 99 (2002) 16331–16335.

[31] T. Braumann, H.L. Grimm, Reversed-phase high-performance liquid chromatography of chlorophyll and carotenoids, Biochim. Biophys. Acta 637 (1981) 1–8.

[32] R. Finsy, Particle sizing by quasi-elastic light scattering, Adv. Colloid Interface Sci. 52 (1994) 79–143.

[33] S. Yedgar, Y. Barenholz, V.G. Cooper, Molecular weight, shape and structure of mixed micelles of triton X-100 and sphingomyelin, Biochim. Biophys. Acta 363 (1974) 98–111.

[34] A. Hager, Ausbildung von maxima im absorptionsspektrum von carotinoiden im bereich um 370 nm; Folgen für die interpretation bestimmter wirkungsspektren, Planta 91 (1970) 38–53.

[35] A.V. Ruban, P. Horton, A.J. Young, Aggregation of higher plant xanthophylls: differences in absorption spectra and in the dependency

on solvent polarity, J. Photochem. Photobiol., B Biol. 21 (1993) 229–234.
[36] F. Zsila, Z. Bikadi, J. Deli, M. Simonyi, Chiral detection of carotenoid assemblies, Chirality 13 (2001) 446–453.
[37] F. Zsila, Z. Bikadi, Z. Keresztes, J. Deli, M. Simonyi, Investigation of the self-organization of lutein and lutein diacetate by electronic absorption, circular dichroism spectroscopy, and atomic force microscopy, J. Phys. Chem., B 105 (2001) 9413–9421.
[38] M. Kasha, Energy transfer mechanisms and the molecular exciton model for molecular aggregates, Rad. Res. 20 (1963) 55–71.
[39] H. Billsten, V. Sundström, T. Polivka, Self-assembled aggregates of the carotenoid zeaxanthin: time resolved study of excited states, J. Phys. Chem., A 109 (2005) 1521–1529.
[40] M.D. Cohen, E. Fischer, Isosbestic points, J. Chem. Soc. 1962 (1962) 3044–3052.
[41] A. Scherz, V. Rosenbach-Belkin, Comparative study of optical absorption and circular dichroism of bacteriochlorophyll oligomers in Triton X-100, the antenna pigment B850, and the primary donor P-860 of photosynthetic bacteria indicates that all are similar dimers of bacteriochlorophyll a, Proc. Natl. Acad. Sci. U. S. A. 86 (1989) 1505–1509.
[42] A. Scherz, V. Rosenbach-Belkin, J.R.E. Fisher, Distribution and self-organization of photosynthetic pigments in micelles: implication for the assembly of light-harvesting complexes and reaction centers in the photosynthetic membrane, Proc. Natl. Acad. Sci. U. S. A. 87 (1990) 5430–5434.
[43] G. Searle, S.S. Brody, A. Van Hoek, Evidence for the formation of a chlorophyll a/zeaxanthin complex in a lecithin liposomes from fluorescence decay kinetics, Photochem. Photobiol. 57 (1990) 401–407.
[44] R. Goss, G. Garab, Non-photochemical chlorophyll fluorescence quenching and structural rearrangements induced by low pH in intact cells of chlorella fusca (Chlorophyceae) and montaniella squamata (Prasinophyceae), Photosyn. Res. 67 (2001) 185–197.
[45] R. Standfuss, A.C.T. van Scheltinga, M. Lamborghini, W. Kuhlbrandt, Mechanisms of photoprotection and nonphotochemical quenching in pea light-harvesting complex at 2.5A resolution, EMBO J. 24 (2005) 919–928.